

Aya M.H. Kinaanah*
Raad M.S. AL-Haddad

Department of Physics,
College of Science,
University of Baghdad,
Baghdad, IRAQ

* Corresponding author email:
Aya.Hasan2304@sc.uobaghdad.edu.iq



Effects of pH Level and Mixing Time on Characteristics of Bismuth Nanoparticles Prepared by Green Synthesis

In this study, bismuth nanoparticles were prepared by green synthesis from Iraqi lemon extract. Results showed that bismuth nanoparticles show absorption peaks at 268-289nm confirming the formation of bismuth nanoparticles with blue shift range. The X-ray diffraction (XRD) analysis confirmed the polycrystalline structure of bismuth nanoparticles with crystallite size of 9-20nm. These nanoparticles have nearly spherical forms with varying diameters between 22.37 and 20.89nm. The zeta potential were estimated to be -43.5 mV and -40 mV confirming the stability of bismuth nanoparticles. The sp^2 hybridization of bismuth nanoparticles was confirmed using Fourier-transform infrared (FTIR) spectrum, from O-H stretching vibrations bonds.

Keywords: Bismuth nanoparticles; Green synthesis; Zeta potential; Iraqi lemon extract
Received: 23 August 2024; Revised: 3 November 2024; Accepted: 10 November 2024; Published: 1 July 2026

1. Introduction

Environmental green method is considered to play an important role in nanoparticle synthesis because it is economical, environmentally friendly and attracts great attention in the medical fields. The nanoparticles prepared in this way are often more stable. Preparing nanoparticles by green method does not require high temperature, energy and high pressure. The green-synthesized nanoparticles have more stability compared to other methods [1-3]. Nanoparticles are shaped like a sphere just a few nanometers in diameter from a huge array of atoms [4]. The preparation and description processing of nanoparticles are appearing and strongly increasing [5]. The important reasons for the popularity of green synthesis are the use of non-toxic materials [6]. The damage in living system results in a functional problem that requires diagnosis [7]. So nanoparticles are entered in many medical physics applications, as well as in optical devices and display screens [8]. In the future, organic materials may be used more than inorganic materials due to the efficiency of their properties [9]. Lemon fruit contains elements that help reduce oxidation, such as limuloids, phenols and various vitamins and acids, such as ascorbic and citric, which work to reduce large oxidation ions. It is an environmentally friendly way to generate bismuth nanoparticles from lemon juice for reducing and coating [10]. The production of nanoparticles must be inexpensive, accepted by society, and not harm the environment [11]. The purpose of this work is to prepare bismuth nanoparticles by the green method and study the effect of pH and time on its properties.

2. Experimental Part

Iraqi lemon was bought from the local market in December 2023. In the first step, about 186.06g of

lemon fruits was collected and thoroughly cleaned with deionized distilled water to get rid of dust, then it was dried and sterilized with ethanol to prepare lemon extract as shown in Fig. (1). In the second step, about 75 ml of lemon juice was mixed with 25 ml of deionized distilled water and put on a magnetic stirrer set to 60°C for 23 min, then collected by centrifugation at 9330 rpm for 10 min to produce the extract and finally stored at 4°C for utilization.

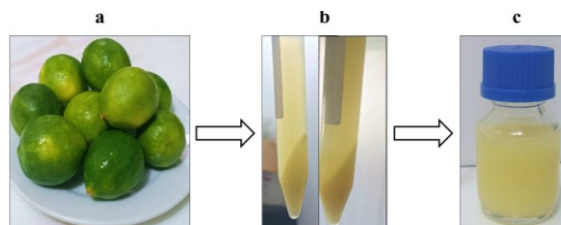


Fig. (1) Iraqi lemon extract synthesis (a) Iraqi lemon fruits,(b) centrifugation,(c) finally product

To obtain the aqueous solution of bismuth nitrate, about 0.023g of $Bi(NO_3)_3 \cdot 5H_2O$ was mixed with 50ml of deionized distilled water at room temperature and constantly stirring for 180 min. The pH was selected to 9–12 using aqueous sodium hydroxide (3.5–4 ml). To obtain the aqueous solution of catalytic reduction about 0.08g of $NaBH_4$ was mixed with 25 ml of deionized distilled water. Finally, to form bismuth nanoparticles, 3ml of Iraqi lemon extract was combined with the aqueous solution of bismuth nitrate.

The primary yellow solution converted into dark orange and finally became dark gray or black, as shown in Fig. (2). The Bismuth nanoparticles were obtained in different color gradations, including black, dark gray, and light gray, depend on the variation in pH and mixing time shown in Figs. (3) and (4).

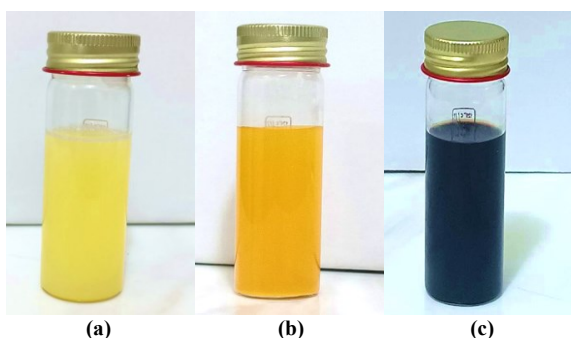


Fig. (2) Bi NPs synthesis at (a) 14 min, (b) 145 min, and (c) 180 min

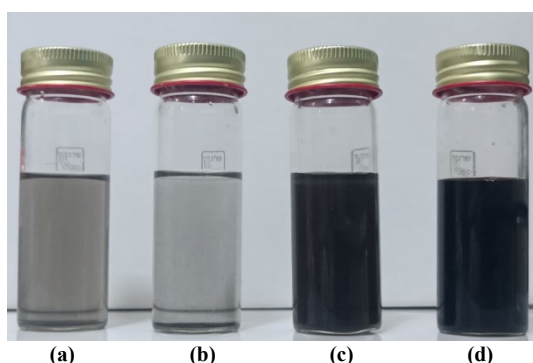


Fig. (3) Bi NPs synthesis with pH variation (a) 9, (b) 10, (c) 11, and (d) 12

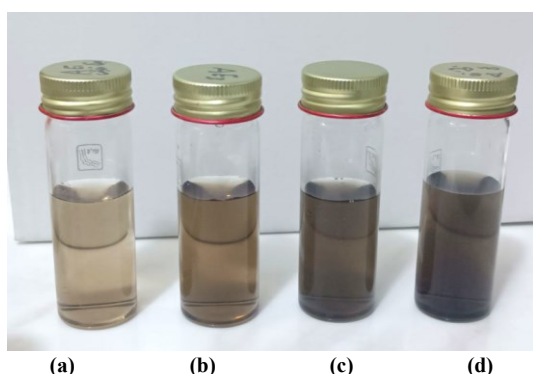


Fig. (4) Bi NPs with time variation (a) 195 min, (b) 90 min, (c) 180 min, and (d) 255 min

The UV-visible spectroscopy was used to determine the absorption peak positions. The X-ray diffraction (XRD) analysis was used to determine the crystalline structure. The stability of prepared bismuth nanoparticles were measured using zeta potential. FTIR was used to determine the electronic structure. The shape and particle size were determined using FESEM. All the techniques mentioned have been applied to of optimum prepared samples at pH of 9 and mixing time of 195 min.

3. Results and Discussion

UV-visible analysis was used to measure the optical characteristics of the synthesized Bi NPs. The absorption spectrum shows a peaks at the range between 268-289nm, as seen in Figs. (5) and (6). The

blue shifted peaks at 268,269,272 and 283 nm under PH variation effect and 280,285,288 289nm under time variation effect proved that bismuth nanoparticles have small size. This result is in good agreement to previously published results by [12]. The peak position of Bi NPs were graphed as functions of each PH and time variation, as shown in Figs. (7) and (8), confirms to the harmony between the wavelength of the incident wave and the standing wave.

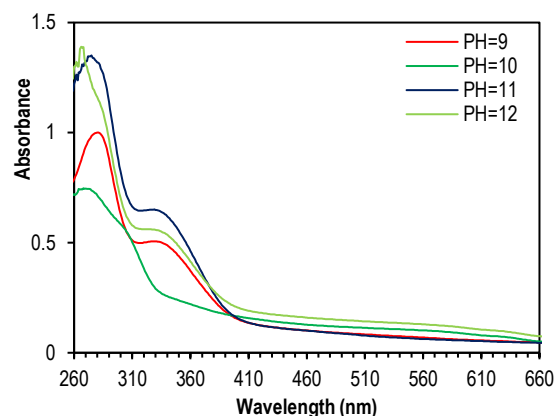


Fig. (5) UV-visible spectra of Bismuth nanoparticles under pH variation effect

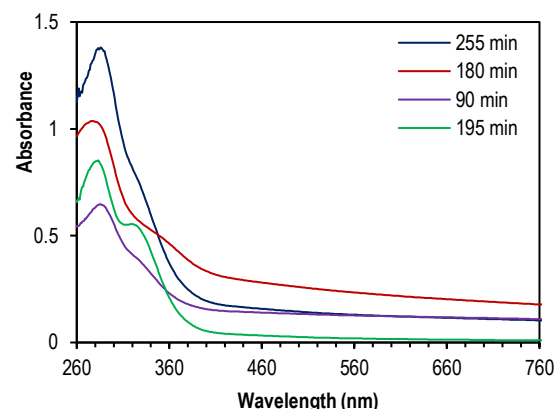


Fig. (6) UV-visible spectra of bismuth nanoparticles under time variation effect

The structural characteristics of the bismuth nanoparticles were studied by XRD as illustrated in Figs. (9) and (10) while tables (1) and (2) show the structural parameters. The average crystallite size of the bismuth nanoparticles was evaluated using Scherer's formula to be 9-20nm. The different peaks were also seen confirms the polycrystalline structure of bismuth nanoparticles. This result is in good agreement to previously published results by [13] and [14].

The zeta potential as illustrated in Figs. (11) and (12) is estimated to be -43.5 mV and -40 mV. This result indicating that the good stability of Bi NPs and directly affected by crystallite size and concentration, as shown in Figs. (13) and (14).

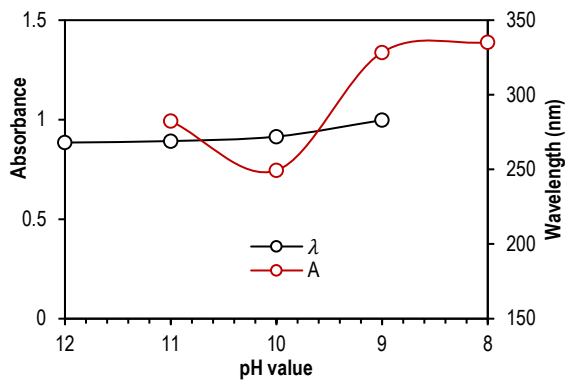


Fig. (7) Optimum peak position of Bi NPs under pH=9 condition

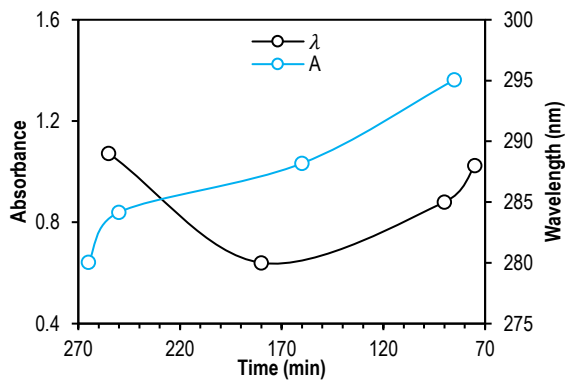


Fig. (8) Optimum peak position of Bi NPs under time =195 min condition

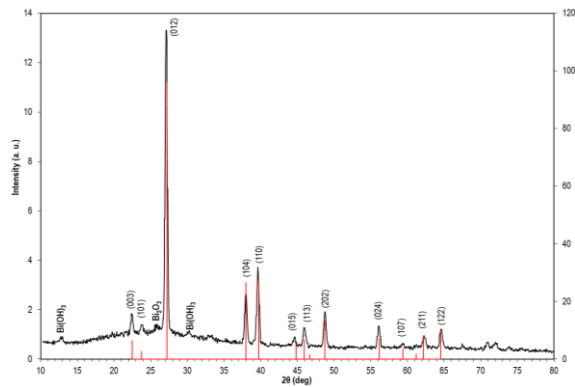


Fig. (9) XRD pattern of bismuth nanoparticles for optimum pH=9

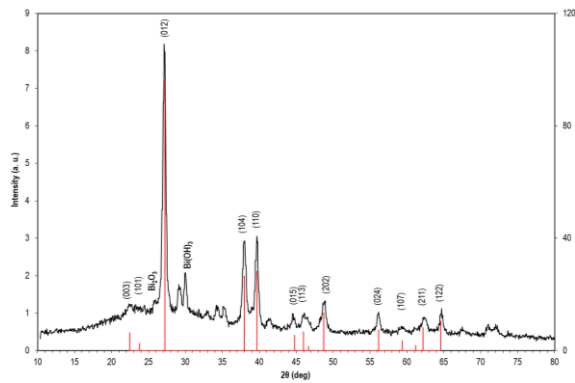


Fig. (10) XRD pattern of bismuth nanoparticles for optimum time =195 min

Table (1) Bi NPs crystallite size with optimum PH condition

| 2θ (deg) | FWHM (deg) | Dhl Exp. (Å) | G.S. (nm) | (hkl) |
|----------|------------|--------------|-----------|-------|
| 22.4168 | 0.4150 | 3.9629 | 19.5 | (003) |
| 23.7574 | 0.4149 | 3.7422 | 19.6 | (101) |
| 27.109 | 0.4149 | 3.2867 | 19.7 | (012) |
| 37.9936 | 0.4149 | 2.3664 | 20.3 | (104) |
| 39.5896 | 0.4469 | 2.2746 | 18.9 | (110) |
| 44.6648 | 0.4150 | 2.0272 | 20.7 | (015) |
| 45.9736 | 0.5745 | 1.9725 | 15.0 | (113) |
| 48.7825 | 0.5745 | 1.8653 | 15.2 | (202) |
| 56.0921 | 0.4469 | 1.6383 | 20.1 | (024) |
| 62.2526 | 0.5107 | 1.4902 | 18.2 | (211) |
| 64.6147 | 0.5107 | 1.4413 | 18.4 | (122) |

Table (2) Bi NPs crystallite size with optimum time condition

| 2θ (deg) | FWHM (deg) | Dhl Exp. (Å) | G.S. (nm) | (hkl) |
|----------|------------|--------------|-----------|-------|
| 22.4459 | 0.6392 | 3.9578 | 12.7 | (003) |
| 27.1216 | 0.6055 | 3.2852 | 13.5 | (012) |
| 37.9529 | 0.5718 | 2.3688 | 14.7 | (104) |
| 39.7021 | 0.4709 | 2.2684 | 17.9 | (110) |
| 44.5123 | 0.4709 | 2.0338 | 18.2 | (015) |
| 45.9923 | 0.8746 | 1.9717 | 9.9 | (113) |
| 48.8179 | 0.6055 | 1.8640 | 14.4 | (202) |
| 56.1509 | 0.5719 | 1.6367 | 15.7 | (024) |
| 62.3066 | 0.7064 | 1.4890 | 13.1 | (211) |
| 64.6276 | 0.5718 | 1.4410 | 16.4 | (122) |

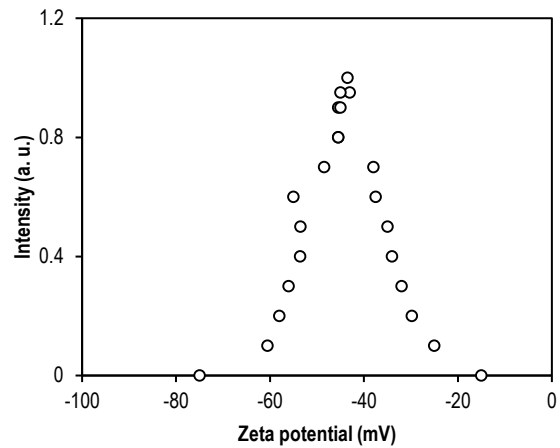


Fig. (11) Zeta potential peak position estimated to be -43.5 mV at pH=9

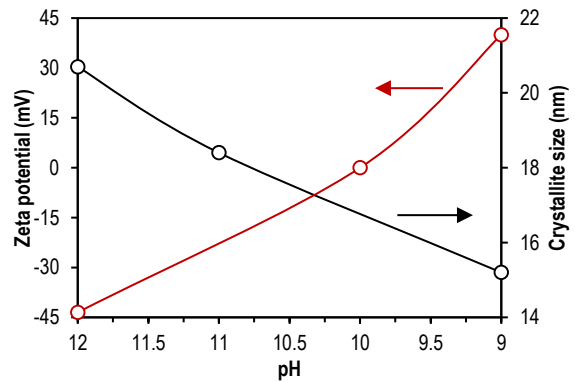


Fig. (12) Zeta potential and crystallite size of uncoated Bi NPs as functions of pH

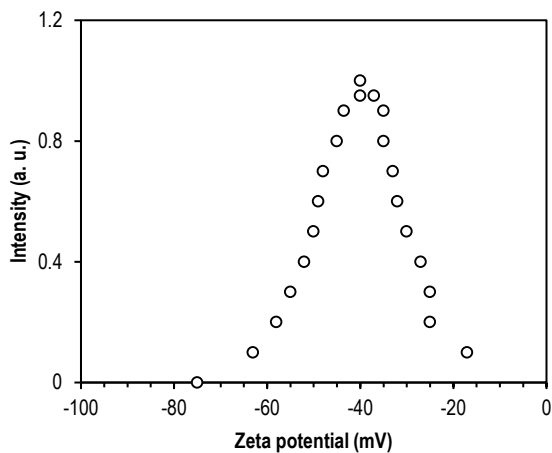


Fig. (13) Zeta potential peak position estimated to be -40 mV at time=195min

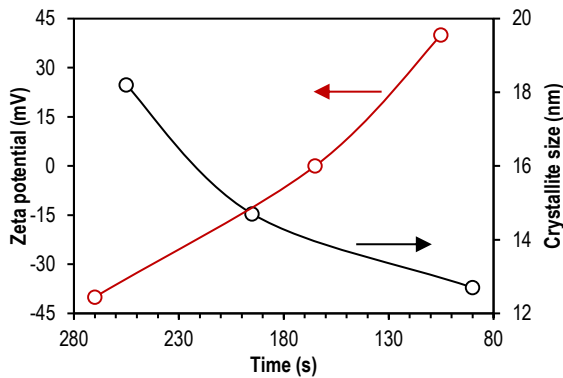


Fig. (14) Zeta potential and crystallite size of uncoated Bi NPs as functions of time

Two types of functional groups on the surface of nanostructures were identified by FTIR spectrum, as illustrated in Fig. (15). This spectrum showed characteristic vibrating modes with wave numbers of 3424.50 cm^{-1} O-H stretching associated with a Carboxyl acid group in sp_2 hybridization, 2501.67 cm^{-1} , 1544.74 cm^{-1} O-H stretch which are attributed to carboxylic acid, 1382.10 cm^{-1} of NO_3^- , 1028.67 cm^{-1} of NO_3^- , 872.285 cm^{-1} Bi-O, 834.752 cm^{-1} Bi-O, 712.772 cm^{-1} Bi-O stretching and 528.236 cm^{-1} Bi-O-Bi bending, indicated that the prepared Bi NPs carried a carboxylic acid functional group on their surfaces. In addition to the presence of the main phytochemicals, which include sugars, fatty acid, phenols, flavonoids and citric acid, in lemon juice extract.

The FTIR spectrum in Fig. (16) shows different peaks with wavenumbers of 3419.53 cm^{-1} O-H stretching associated with a carboxyl acid group in sp_2 hybridization, 2505.53 cm^{-1} , 1563.61 cm^{-1} O-H stretch which are attributed to carboxylic acid, 1382.54 cm^{-1} of NO_3^- , other functional groups at the range 1200-400 involve sp_2 hybridization including: 1028.4 cm^{-1} of NO_3^- , 868.639 cm^{-1} Bi-O, 834.024 cm^{-1} Bi-O, 711.538 cm^{-1} Bi-O Stretching and 522.485 cm^{-1} Bi-O-Bi bending, group in sp_2 hybridization, This type of hybridization indicates the metallic properties of

Bismuth nanoparticles. This result is in good agreement to previously published results by [15].

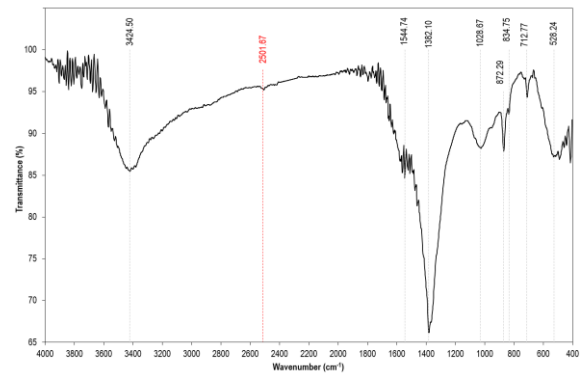


Fig. (15) FTIR spectrum of bismuth nanoparticles with pH=9

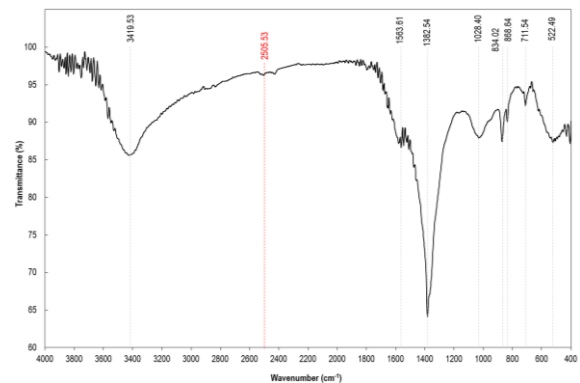
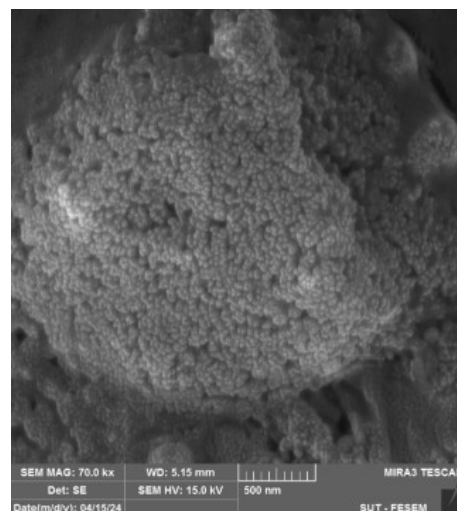


Fig. (16) FTIR spectrum of bismuth nanoparticles with 195 min

The shape and diameter were measured using field emission scanning electron microscopy as shown in Figs. (17) and (18). The FE-SEM image demonstrates the uniform distribution of grains and approximately spherical morphologies of the bismuth nanoparticle, which range in diameter from 20.89 to 22.37 nm.



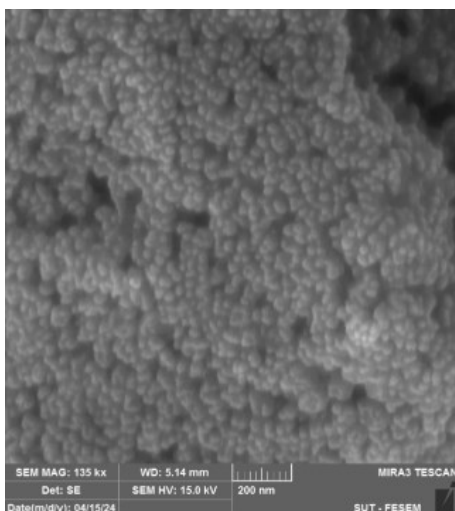


Fig. (17) FE-SEM images of bismuth nanoparticles with optimum pH =9

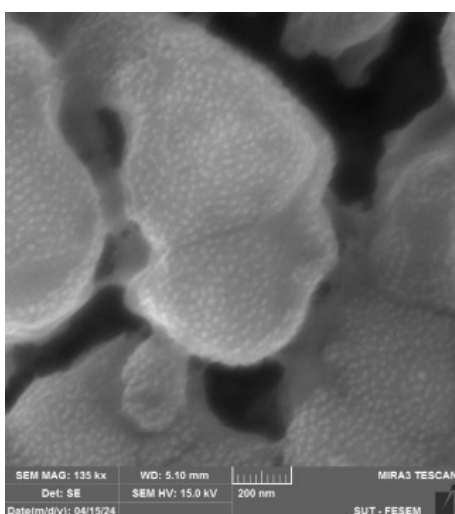
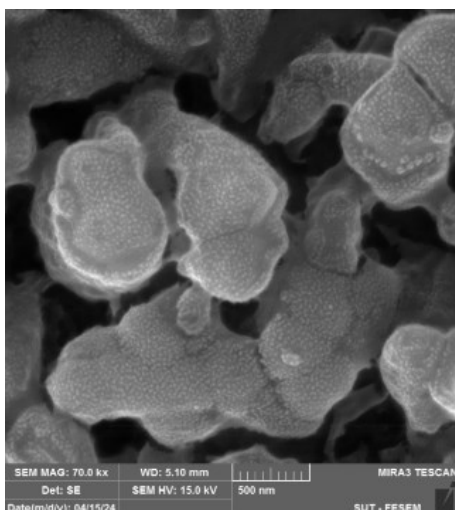


Fig. (18) FE-SEM images of bismuth nanoparticles with optimum time =195min

4. Conclusion

The green method has been proven effective in preparing bismuth nanoparticles. UV-visible spectra demonstrated the absorbance peak positions are shifting to the blue shift suggests a decrease in particle size. XRD pattern showed the metallic purity of Bi NPs. FTIR spectra showed different peaks with wave numbers at sp_2 hybridization. FESEM analysis confirmed the small size and uniform shape. The Zeta potential is estimated to be -43.5 mV and -40 mV indicates an increase in bismuth nanoparticles stability.

References

- [1] R.M. Abdallah and R.M. Al-Haddad, "Optical and Morphology Properties of the Magnetite (Fe_3O_4) Nanoparticles Prepared by Green Method", *J. Phys.: Conf. Ser.*, 1829(1) (2021) 1-9.
- [2] G.E. Hoag et al., "Degradation of bromothymol blue by 'greener' nano-scale zero-valent iron synthesized using tea polyphenols", *J. Mater. Chem.*, 19(45) (2009) 8671-8677.
- [3] T. Shahwan et al., "Green synthesis of iron nanoparticles and their application as a Fenton-like catalyst for the degradation of aqueous cationic and anionic dyes", *Chem. Eng. J.*, 172(1) (2011) 258-266.
- [4] H.N. Noori and A.F. Abdulameer, "Study of the Optical Properties of 3MPA CdTe and 3MPA CdTe/CdSe Quantum Dots at pH 12 in Different Periods of Time", *Iraqi J. Phys.*, 21(4) (2023) 77-83.
- [5] N.K. Abass et al., "Fabricated of Cu Doped ZnO Nanoparticles for Solar Cell Application", *Baghdad Sci. J.*, 15(2) (2018) 198-204.
- [6] A.H. Fezaa, R.M.S. Al-Haddad and A.M. Ali, "Licorice-Based Biosynthesis of Gold Nanoparticles and Evaluation of Some Pathogenic Bacteria's Resistance to Antibacterial Agents", *Int. J. Nanosci.*, 22(5) (2023) 2350039.
- [7] H.N. Noori and A.F. Abdulameer, "A Review of Biosensors; Definition, Classification, Properties, and Applications", *Iraqi J. Sci.*, 64(11) (2023) 5665-5690.
- [8] H.N. Noori and A.F. Abdulameer, "Study of the Effect of pH on the Optical Properties of the CdTe Quantum Dots", *Iraqi J. Sci.*, 64(2) (2023) 653-657.
- [9] H.N. Noori and L.K. Abbas, "Annealing effect on the optical properties of organic semiconductor Alq3:C60 blend thin films", *Iraqi J. Phys.*, 16(39) (2018) 1-10.
- [10] M.d. Mahiuddin and B. Ochiai, "Green synthesis of crystalline Bismuth nanoparticles using lemon juice", *Royal Soc. Chem.*, 11(43) (2021) 26683-26686.
- [11] S. Saif, A. Tahir and Y. Chen, "Green synthesis of iron nanoparticles and their environmental

- applications and implications”, *Nanomater.*, 6(11) (2016) 1-26.
- [12] S.S. Hassan, R.M.S. Al-Haddad and K.A. Hubeatir, “Temperature Effects on the Optical Properties of Bismuth Nanoparticles Prepared by PLAL for Antibacterial Activity”, *Int. J. Nanoelectron. Mater.*, 16 (2022) 1-12.
- [13] Md. Mahiuddin and Bungo Ochiai, “Comprehensive Study on Lemon Juice-Based Green Synthesis and Catalytic Activity of Bismuth Nanoparticles”, *ACS Omega*, 7(40) (2022) 35626-35634.
- [14] S.S. Hassan, K.A. Hubeatir and R.M.S. Al-Haddad, “Characterization and antibacterial activity of silica-coated bismuth (Bi@SiO₂) nanoparticles synthesized by pulsed laser ablation in liquid”, *Optik*, 273 (2023) 170453.
- [15] P. Nazari et al., “The Antimicrobial Effects and Metabolomic Footprinting of Carboxyl-Capped Bismuth Nanoparticles against *Helicobacter pylori*”, *Appl. Biochem. Biotech.*, 172 (2014) 570-579.
-